Steric asymmetry and lambda-doublet propensities in state-to-state rotationally inelastic scattering of NO($^2\Pi_{1/2}$) with He

Marc J. L. de Lange[a] and Steven Stolte[b]
Laser Centre and Department of Physical Chemistry, Faculty of Exact Sciences, Vrije Universiteit, De Boelelaan 1083, 1081 HV Amsterdam, The Netherlands

Craig A. Taatjes
Combustion Research Facility, Mail Stop 9055, Sandia National Laboratories, Livermore, California 94551

Jacek Kłos,[c] Gerrit C. Groenenboom, and Ad van der Avoird
Institute of Theoretical Chemistry, NSRIM, University of Nijmegen, Toernooiveld 1, 6526 ED Nijmegen, The Netherlands

(Received 10 August 2004; accepted 24 September 2004)

Relative integrated cross sections are measured for rotationally inelastic scattering of NO($^2\Pi_{1/2}$), hexapole selected in the upper Λ-doublet level of the ground rotational state ($j=0.5$), in collisions with He at a nominal energy of 514 cm^{-1}. Application of a static electric field $\mathbf{E}$ in the scattering region, directed parallel or antiparallel to the relative velocity vector $\mathbf{v}$, allows the state-selected NO molecule to be oriented with either the N end or the O end towards the incoming He atom. Laser-induced fluorescence detection of the final state of the NO molecule is used to determine the experimental steric asymmetry, $\mathrm{SA}\equiv(\sigma_{\mathbf{v}\uparrow\downarrow\mathbf{E}}-\sigma_{\mathbf{v}\uparrow\uparrow\mathbf{E}})/(\sigma_{\mathbf{v}\uparrow\downarrow\mathbf{E}}+\sigma_{\mathbf{v}\uparrow\uparrow\mathbf{E}})$, which is equal to within a factor of (-1) to the molecular steric effect, $S_{i\rightarrow f}\equiv(\sigma_{\mathrm{He}\rightarrow\mathrm{NO}}-\sigma_{\mathrm{He}\rightarrow\mathrm{ON}})/(\sigma_{\mathrm{He}\rightarrow\mathrm{NO}}+\sigma_{\mathrm{He}\rightarrow\mathrm{ON}})$. The dependence of the integral inelastic cross section on the incoming Λ-doublet component is also observed as a function of the final rotational (j'), spin-orbit (Ω'), and Λ-doublet (ϵ') state. The measured steric asymmetries are significantly larger than previously observed for NO-Ar scattering, supporting earlier proposals that the repulsive part of the interaction potential is responsible for the steric asymmetry. In contrast to the case of scattering with Ar, the steric asymmetry of NO-He collisions is not very sensitive to the value of Ω'. However, the Λ-doublet propensities are very different for $[\Omega=0.5(F_1)\rightarrow\Omega'=1.5(F_2)]$ and $[\Omega=0.5(F_1)\rightarrow\Omega'=0.5(F_1)]$ transitions. Spin-orbit manifold conserving collisions exhibit a propensity for parity conservation at low Δj, but spin-orbit manifold changing collisions do not show this propensity. In conjunction with the experiments, state-to-state cross sections for scattering of oriented NO($^2\Pi$) molecules with He atoms are predicted from close-coupling calculations on restricted coupled-cluster methods including single, double, and noniterated triple excitations [J. Klos, G. Chalasinski, M. T. Berry, R. Bukowski, and S. M. Cybulski, J. Chem. Phys. **112**, 2195 (2000)] and correlated electron-pair approximation [M. Yang and M. H. Alexander, J. Chem. Phys. **103**, 6973 (1995)] potential energy surfaces. The calculated steric asymmetry $S_{i\rightarrow f}$ of the inelastic cross sections at $E_{tr}=514\,\mathrm{cm}^{-1}$ is in reasonable agreement with that derived from the present experimental measurements for both spin-manifold conserving ($F_1\rightarrow F_1$) and spin-manifold changing ($F_1\rightarrow F_2$) collisions, except that the overall sign of the effect is opposite. Additionally, calculated field-free integral cross sections for collisions at $E_{tr}=508\,\mathrm{cm}^{-1}$ are compared to the experimental data of Joswig *et al.* [J. Chem. Phys. **85**, 1904 (1986)]. Finally, the calculated differential cross section for collision energy $E_{tr}=491\,\mathrm{cm}^{-1}$ is compared to experimental data of Westley *et al.* [J. Chem. Phys. **114**, 2669 (2001)] for the spin-orbit conserving transition $F_1\,(j=0.5)\rightarrow F_1 f\,(j'=3.5)$. © *2004 American Institute of Physics.* [DOI: 10.1063/1.1818123]

I. INTRODUCTION

The inelastic scattering of open-shell molecules is a source of detailed information about energy exchange during evolution on coupled surfaces. Scattering of NO from rare gas atoms has served as a convenient prototype for investigations of open-shell molecular energy transfer. The spectroscopy of NO is well-developed and state-specific detection of scattered products is readily achievable. Additionally, it is possible to select a single rotational and Λ-doublet state of NO from a molecular beam with a hexapole state selector, and subsequently to orient the axis of the state-selected NO molecule in the laboratory frame by application of a static electric field.[1–4] Scattering from such a prepared state permits the measurement of the steric asymmetry in inelastic

[a]Present address: Molecular Cytology, Swammerdam Institute for Life Sciences, University of Amsterdam, P.O. Box 94062, 1090 GB Amsterdam, The Netherlands.
[b]Author to whom correspondence should be addressed. Electronic mail: stolte@few.vu.nl
[c]Author to whom correspondence should be addressed, Department of Chemistry and Biochemistry, University of Maryland, College Park, MD 20742. Electronic mail: jklos@mail.umd.edu

scattering, that is, the difference in scattering efficiency between collisions on the N and O ends of the molecule.[4–6]

The NO-Ar system has been the most thoroughly investigated of the NO rare gas collision systems. State-specific integral[7–12] and differential[13–17] cross section measurements for inelastic scattering of ground state NO have been compared with high-level quantum calculations,[16–18] and the vector correlations in the final products mapped in exquisite detail.[19–21] The steric asymmetry for spin-orbit conserving scattering of NO-Ar shows striking oscillations with Δj; for Δj even, collisions with the N end of the molecule are preferred, and for Δj odd, collisions with the O end are more effective.[5,6] Although it is reproduced in quantum scattering calculations[5,22,23] (to within the overall sign of the effect[24]), there is at present no simple physical picture of the source of this alternation. Examination of the *T*-matrix description of the collision process shows that the difference between scattering from the N and O end of the molecule is dependent on interference terms between transitions from *e* and *f* initial Λ-doublet levels.[5,22] The alternation between even and odd Δj is reminiscent of other interference effects in near-homonuclear molecules.[9,25] Calculation of the steric effect in rotationally inelastic collisions of NO and Ar on modified test potentials suggests that scattering from the repulsive core is most important in producing the alternation with Δj.[23]

The present work investigates steric effects in inelastic scattering of NO and He, a system where repulsive interactions dominate. Much is already known about NO-He scattering, although it has been less comprehensively studied than NO-Ar. Integral and differential cross sections for NO-He scattering have been measured by several groups. Using crossed molecular beams and laser-induced fluorescence (LIF) detection, Joswig, Andresen, and Schinke[10] determined state-resolved integral cross sections for NO scattering from rare gas partners. Meyer[26] scattered counter-propagating beams of NO and He and detected the inelastically scattered products with resonant multiphoton ionization and ion time-of-flight analysis. He derived state-resolved relative integral and differential cross sections and measured angular momentum alignment of the products.[27] Chandler and co-workers[28] measured differential cross sections for scattering of initially cold NO($^2\Pi_{1/2}$) to individual final rotational and Λ-doublet levels in both the $^2\Pi_{1/2}$ and $^2\Pi_{3/2}$ manifolds. Smith and co-workers[8] used a rotating-source crossed molecular beam apparatus to measure final rotational state populations for NO-He and NO-Ar inelastic scattering as a function of collision energy. State-to-state rate coefficients for rotational energy transfer in vibrationally excited NO rare gas collisions have been measured by Smith's group[29–31] at temperatures down to 7 K and for the ground vibrational state by Ball and De Lucia at 4.2 K.[32] Drabbels *et al.*[33] measured parity-resolved state-to-state cross sections for scattering of NO ($v=20$, $j=0.5$) and compared to close-coupled scattering calculations on the correlated electron-pair approximation (CEPA) surface of Yang and Alexander.[34] More recently another *ab initio* He-NO surface has been calculated by Kłos *et al.*[35] using restricted coupled-cluster methods including single, double, and noniterated triple excitations [RCCSD(T)]. Alexander[22] calculated steric effects for several inelastic scattering transitions of NO-He using the CEPA surface[34] and predicted large steric asymmetries and oscillations with Δj similar to those seen in NO-Ar scattering.

This work reports the experimental measurements of the steric asymmetry for inelastic scattering of NO($^2\Pi_{1/2}, j=0.5$) with He. Distinct alternations in the sign of the steric asymmetry appear in both spin-orbit changing and spin-orbit conserving transitions. The propensity for Λ-doublet changing or conserving collisions is also measured. The experimental results are compared to quantum scattering calculations on the CEPA surface of Yang and Alexander[34] and the RCCSD(T) surface of Kłos *et al.*[35] Calculations on both surfaces reproduce the experimental results with reasonable accuracy to within the overall sign, with somewhat poorer agreement for spin-orbit changing collisions than for spin-orbit conserving collisions.

II. CALCULATIONS

A. Formalism of oriented molecule scattering

In scattering involving radicals in a $^2\Pi$ state the relative translational motion of the collision partner can change the rotational and also internal electronic motion. The NO molecule in the ground $^2\Pi$ state is split into two spin-orbit components with projection Ω of the total angular momentum on the internuclear axis of $\Omega=0.5$ [labeled in Hund's case (a) as F_1] and $\Omega=1.5$ (labeled as F_2). Then each rotational level is split into two closely separated Λ-doublet levels of spectroscopic parity *e* (symmetry quantum number $\epsilon=+1$) and *f* ($\epsilon=-1$). The total parity *p* is related to ϵ by $\epsilon=p(-1)^{j-S}$, where *S* is the total spin ($S=1/2$). The presence of a structureless collision partner, in this case a He atom, removes the cylindrical degeneracy of the $^2\Pi$ state of the NO molecule. The full description of the collision therefore involves two adiabatic potential energy surfaces, one of A' and one of A'' symmetry with respect to the reflection in the plane of the three atoms.

These adiabatic surfaces are obtained from *ab initio* calculations. The expansion of the potential surfaces for van der Waals complexes between rare gas atoms and molecules in $^2\Pi$ states is described by Alexander[23] and generally in the work of Zeimen *et al.*[36,37] Briefly, the intermolecular potential energy operator *V* is expanded in the set of diabatic states $|\Lambda\rangle$ where the projection of the electronic orbital angular momentum $\Lambda=\pm1$. These diabatic states are components of the Π state and are defined in coordinates (R,θ,ϕ) that specify the position of the He atom relative to the NO center of mass and the molecule-fixed $\hat{z}$ axis pointing from the O atom to the N atom along the molecular bond. The expansions can be written down as follows:

$$\hat{V}=\sum_{\Lambda_1,\Lambda_2}|\Lambda_1\rangle V_{\Lambda_1,\Lambda_2}(R,\theta)\langle\Lambda_2|. \tag{1}$$

The matrix elements $V_{\Lambda_1,\Lambda_2}(R,\theta)$ are the diabatic potential energy surfaces for the He-NO($^2\Pi$) system. These diabatic matrix elements can be expanded in a series of Racah normalized spherical harmonics $C_{lm}(\theta,\phi)$:

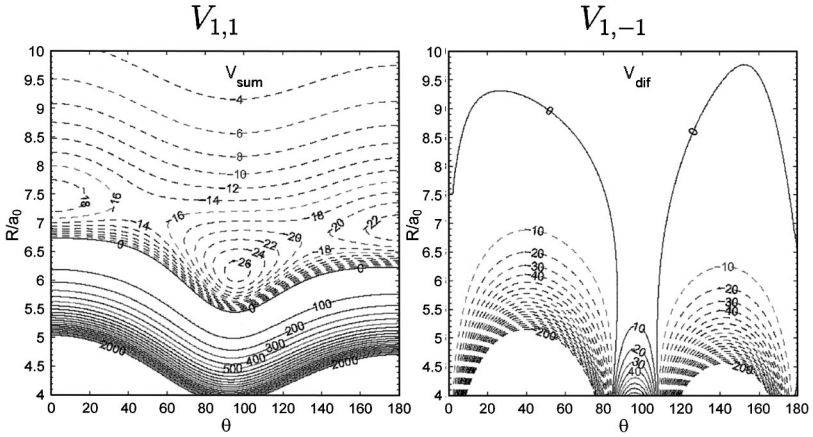

FIG. 1. Contour plots of the sum and difference potentials (energy in cm^{-1}) for NO-He from the RCCSD(T) calculations of Kłos *et al.* (Ref. 35). The angle $\theta=0°$ corresponds to the collinear He-NO configuration and $\theta=180°$ to He-ON. Dashed contours represent attractive regions of the surface and solid contours represent repulsive regions. The dashed contours are spaced by 2 cm^{-1} and the solid contours by 100 cm^{-1} for $V_{1,1}$ (left panel). The contour spacing is 10 cm^{-1} for the difference potential $V_{1,-1}$ (right panel).

$$V_{\Lambda_1,\Lambda_2}(R,\theta)=\sum_{l,m} v^{l,m}_{\Lambda_1,\Lambda_2}(R)C_{lm}(\theta,0). \tag{2}$$

From the invariance properties of the electronic Hamiltonian under rotations of the entire system[36,37] one can derive that all expansion coefficients $v^{l,m}_{\Lambda_1,\Lambda_2}(R)$ vanish except those with $m=\Lambda_2-\Lambda_1$. The connection between the adiabatic potentials of A' and A'' symmetry and the diabatic potentials is

$$\begin{aligned} V_{A'}&=\langle +|V|+\rangle = V_{1,1}-V_{1,-1},\\ V_{A''}&=\langle -|V|-\rangle = V_{1,1}+V_{1,-1}, \end{aligned} \tag{3}$$

where the adiabatic states are given in terms of the diabatic basis by $|A'\rangle=|+\rangle=2^{-1/2}(|-1\rangle-|1\rangle)$ and $|A''\rangle=|-\rangle=2^{-1/2}i(|-1\rangle+|1\rangle)$. For the $^2\Pi$ state of NO it gives nonvanishing diagonal expansion coefficients with $m=0$ and off-diagonal coefficients with $m=\pm 2$.

Using Eqs. (2) and (3) one can obtain the expansion formulas[36,37] for diabatic potentials used in the scattering calculations:

$$\begin{aligned} V_{1,1}(R,\theta)&=\frac{V_{A'}+V_{A''}}{2}=\sum_l v^{l,0}(R)C_{l,0}(\theta,0),\\ V_{1,-1}(R,\theta)&=V_{-1,1}(R,\theta)\\ &=\frac{V_{A''}-V_{A'}}{2}=\sum_l v^{l,-2}(R)C_{l,-2}(\theta,0). \end{aligned} \tag{4}$$

The $V_{1,1}(R,\theta)$ surface is also called V_{sum} and the $V_{1,-1}(R,\theta)$ is called V_{diff}.[23] In the work of Alexander and Stolte[23] the expansion of $V_{1,-1}(R,\theta)$ differs only in the normalization constant of the spherical harmonics. The $V_{1,1}(R,\theta)$ and the $V_{1,-1}(R,\theta)$ surfaces from the RCCSD(T) calculations of Kłos *et al.*[35] are shown in Fig. 1.

The NO($^2\Pi$) molecule can be described in the Hund's coupling case (a), with a relatively large spin-orbit splitting between $^2\Pi_{1/2}$ (ground) and $^2\Pi_{3/2}$ states. The NO spin-orbit splitting is $\Delta_{SO}=123.14\,cm^{-1}$, and the rotational constant of the molecule is $B=1.696\,11\,cm^{-1}$.[38] The states of NO can be expanded in the following basis functions:

$$|\Lambda,S,\Omega,j,m_j\rangle=|\Lambda,S,\Omega\rangle\left[\frac{2j+1}{4\pi}\right]^{1/2}D^{(j)*}_{m_j,\Omega}(\phi_c,\theta_c,0), \tag{5}$$

where the polar and azimuthal angles (θ_c,ϕ_c) describe the orientation of the NO axis with respect to the laboratory collision frame, for which the z axis is chosen parallel to the initial relative velocity vector $\mathbf{v}\equiv(\mathbf{v}_{He}-\mathbf{v}_{NO})=d\mathbf{R}/dt$. The $|\Lambda,S,\Omega\rangle$ basis function describes the electronic angular momentum and spin of the NO molecule. The j denotes the total angular momentum quantum number of NO. The Ω quantum number is the projection of total angular momentum of NO on its internuclear axis and m_j is its projection on the laboratory $\hat{z}$ axis. In this case, $\Lambda=\pm 1$ and $S=1/2$. The elements of the Wigner D matrix describe the rotation of the NO molecule. From this basis one can construct the parity-adapted basis,

$$\begin{aligned} ||\Lambda|,S,\Omega,j,m_j,\epsilon\rangle=2^{-1/2}[&|\Lambda,S,\Omega,j,m_j\rangle\\ &+p(-1)^{j-S}|-\Lambda,S,-\Omega,j,m_j\rangle], \end{aligned} \tag{6}$$

consisting of eigenfunctions of the inversion operator with eigenvalues $p=\pm 1$. The spectroscopic parity ϵ is related to the total parity by $\epsilon=p(-1)^{j-S}$. The basis functions with $\epsilon=+1$ are labeled with the label e and those with $\epsilon=-1$ with the label f. The interaction with other electronic states gives a splitting between states of e and f symmetry, which is called the Λ-doublet splitting, and is on the order of 0.012 cm^{-1} for the $^2\Pi_{1/2}$ ground state of the NO molecule.[35]

The electric field **E**, applied in the experiment to orient NO molecules before collisions with the He beam, mixes field-free states of e and f parity,

$$|j,m_j,\Omega,\pm\mathbf{E}\rangle=\alpha|j,m_j,\Omega,f\rangle\pm\beta|j,m_j,\Omega,e\rangle, \tag{7}$$

with the normalization $\alpha^2+\beta^2=1$ and where the $|\Lambda|=1$ and $S=1/2$ labels are omitted for brevity. The direction of **E** determines which end of the molecule points preferentially towards the He atom. The real mixing parameters α and β are obtained from the solution of a 2×2 Stark mixing Hamiltonian.[39] Similarly, mixing of field-free scattering amplitudes is employed to evaluate the scattering amplitude from the initial mixed state in the presence of the electric field to the final states of NO molecule in the field-free basis:

$$f_{jm_j\Omega\pm\mathbf{E}\to j'm_j'\Omega'\epsilon'}=\alpha f_{jm_j\Omega f\to j'm_j'\Omega'\epsilon'} \pm\beta f_{jm_j\Omega e\to j'm_j'\Omega'\epsilon'}. \quad (8)$$

The calculated integral cross sections from these scattering amplitudes for collisions of oriented NO molecules are used to define the steric asymmetry for the transition from initial state i to final state f:[23,24]

$$S_{i\to f}=\frac{\sigma_{\mathrm{He}\to\mathrm{NO}}-\sigma_{\mathrm{He}\to\mathrm{ON}}}{\sigma_{\mathrm{He}\to\mathrm{NO}}+\sigma_{\mathrm{He}\to\mathrm{ON}}}. \quad (9)$$

The theory applied in these calculations was also presented earlier[23] and incorporated in the HIBRIDON package[40] which is used in this work.

B. Outline of scattering calculations

Full close-coupling calculations are performed for collision energy $E_{tr}=514\,\mathrm{cm}^{-1}$, corresponding to the present experimental conditions. The mixing parameters α and β are $\alpha=0.883$ and $\beta=0.470$. In the initial beam of NO only one state is significantly populated, $j=0.5$ and $\Omega=0.5\,(F_1)$. The hexapole selects the upper state $\epsilon=-1\,(f)$ Λ doublet of NO, so this is chosen as the initial state in the field-free calculation. The average orientation of the NO molecule, given by the mean value of the cosine of the angle $\theta_{\mathbf{E}}$ between the molecular axis and the direction of the applied electric field $\mathbf{E}$, can be expressed as a function of the mixing parameters and the maximum degree of orientation ($\langle\cos\theta_{\mathbf{E}}\rangle_{\max}=1/3$ for a $j=0.5$ state): $\langle\cos\theta_{\mathbf{E}}\rangle=2\alpha\beta\langle\cos\theta_{\mathbf{E}}\rangle_{\max}$. The experimental mixing parameters correspond to an averaged orientation of 83% of the maximum value.

The calculations are performed with the HIBRIDON package[40] using a log-derivative propagator in the radial range $(4.0-12.0)a_0$ with a step size of $0.14a_0$ and an Airy propagator in the long range for $R>120_0$ with a seven-times larger step. To ensure proper convergence of the calculated cross sections the summation over total angular momentum quantum number J_{tot} is carried out up to $J_{\mathrm{tot,max}}=120.5$. All channels of the NO molecule are included up to $j_{\max}=20.5$. Calculations are performed on the recently published coupled-cluster [RCCSD(T)] potential energy surface[35] (PES) and on the older correlated electron-pair approximation (CEPA) PES of Yang and Alexander.[34]

III. EXPERIMENT

The measurements are carried out using a crossed, pulsed, molecular-beam scattering apparatus, similar to that described in earlier studies.[5–7] NO molecules are expanded through a 0.8 mm diameter pulsed (10 Hz) nozzle from a 16% mixture of NO in Ar at a stagnation pressure of 3.5 bar. The skimmed beam passes through a 167 cm long hexapole assembly that focuses the molecules in the selected $|jm_j\Omega\epsilon\rangle=|1/2\pm1/2\ 1/2-1\rangle$ state into the scattering center, 293 cm from the pulsed nozzle source.[6] The NO beam is crossed at 90° by a beam of He, expanded from a stagnation pressure of 3 bar through a 0.9 mm pulsed nozzle at 5 Hz and collimated by a 1.9 mm skimmer placed 1.4 cm from the nozzle. The distance from the He pulsed nozzle to the scattering center is 8.4 cm. The speeds of both beams, $\overline{\mathbf{v}}_{\mathrm{NO}}=594\,\mathrm{m\,s}^{-1}$ and $\overline{\mathbf{v}}_{\mathrm{He}}=1764\,\mathrm{m\,s}^{-1}$, yield a nominal center-of-mass collision energy of $\sim514\ \mathrm{cm}^{-1}$. The state-selected NO molecules are oriented by a $10\ \mathrm{kV\,cm}^{-1}$ dc electric field, applied parallel or antiparallel to the relative velocity vector.[6] This applied field creates a superposition of parity states with a definite laboratory frame orientation; the negatively charged end of the NO molecule points preferentially towards the negative electrodes. The coefficients describing this superposition have been experimentally deduced from measurements of LIF intensities of field-induced transitions.[4]

The scattered NO molecules are monitored as a function of final quantum state via LIF, using the frequency doubled ($\sim$226 nm) output of a Nd:YAG (YAG—yttrium aluminum garnet) pumped dye laser operating at 10 Hz. The pulse energy of the laser is typically several hundreds of microjoules and the frequency bandwidth is $0.15\ \mathrm{cm}^{-1}$ (full width at half maximum). The propagation direction and the linear polarization of the laser lie in the plane of the molecular beams; the laser makes an angle of $\sim30°$ with the relative velocity vector. The fluorescence is collected perpendicular to the plane of the molecular and laser beams, filtered by a cell of liquid CH_2Cl_2, and imaged onto a solar-blind photomultiplier tube (PMT). The PMT voltage can be gated in time to discriminate against scattered laser light.

The output of the PMT is collected by a gated integrator and boxcar averager, and transferred to a personal computer (PC). The repetition rate of the secondary beam is half of that of the NO beam and of the laser so that the signal with and without the He beam is measured on alternate laser shots. The subtraction of the scattered signal and the baseline signal, yielding the LIF signal for molecules scattered from the prepared initial state to the probed final state $|j'\Omega'\epsilon'\rangle$, is carried out for successive pairs of laser shots in the PC. After 100 pairs of laser pulses in the absence of the orientation field (probing the scattered signal of the pure upper Λ-doublet component), voltage is applied to the orientation electrodes. The scattered signal at one orientation is then collected for 100 pairs of pulses, followed by reversal of the orientation field, a pause of 2 s, and collection of signal for 100 pairs of pulses at the opposite direction. Finally the voltage of the orientation field is again set to 0 kV. This cycle is repeated 12–15 times. To eliminate possible bias if the determination of the scattered signal for one orientation was always preceded by the zero field measurements, the order of the measurements of the two orientations is switched on alternate cycles. For the selected state, with a positive Stark effect, the positively charged end of the molecule will point towards the positive electrode. With the electric field defined as pointing from positive to negative polarity, the relative LIF signals for the two orientations of the electric field, $I(\mathbf{v}\uparrow\uparrow\mathbf{E})\equiv I^+$ and $I(\mathbf{v}\uparrow\downarrow\mathbf{E})\equiv I^-$, are proportional to the relative inelastic cross sections for collisions of He with the positive and negative end of the NO dipole.

The apparatus function relating the relative LIF intensities to relative inelastic scattering cross sections has been evaluated based on the geometry and beam velocities of the present experimental configuration.[41] The measurement of the steric effect is insignificantly affected by the apparatus

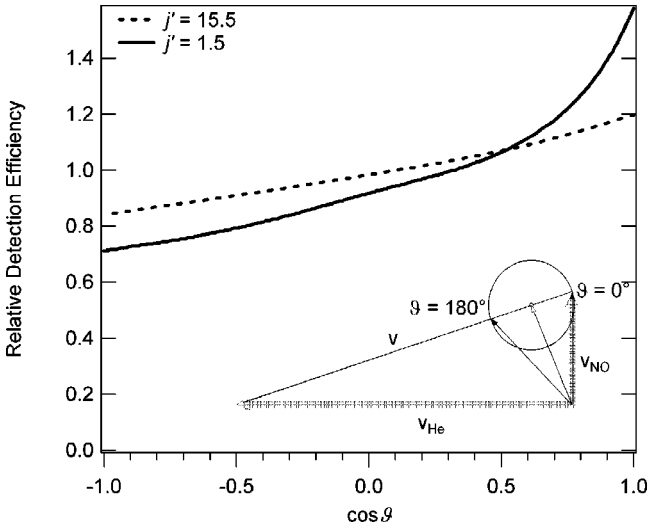

FIG. 2. The normalized calculated relative LIF detection probability as a function of center-of-mass scattering angle ϑ for scattered NO molecules in final state $F_1(j'=1.5)$ (solid line) and $F_1(j'=15.5)$ (dashed line) in the present experimental arrangement. The inset shows a Newton diagram for the experiment, with a Newton sphere corresponding to a nearly-elastic collision.

function, because most possible confounding factors relate to the dependence of the final velocity on the scattering angle and are insensitive to the direction of the electric field. The apparatus function slightly favors detection of forward scattered products, as shown in Fig. 2, but the field-dependent ratio of LIF signals should still closely approximate the angle-averaged steric asymmetry. Effects of the polarized laser detection are expected to be minimal, despite the fact that the angular momentum vector of the scattered product may be aligned.[21,26,27] The detection probability using linear polarization, even for anisotropic final m_j' distributions, should be invariant to a change in the direction of the dc field. It is possible that detection on different rotational transitions could preferentially probe different scattering angles because of product alignment, and provide a glimpse of possible scattering-angle dependent steric effects. However, measurements of steric effects on Q and P, R branches showed no significant systematic variation under the present (partially saturated) conditions. More sophisticated measurements will be required to obtain information on orientation-resolved differential cross sections.

The experimentally accessible steric effect is given by the difference between the LIF signals for opposite orientations of the static field, normalized by their sum:

$$\mathrm{SA} \equiv \frac{\sigma_{\mathbf{v}\uparrow\downarrow\mathbf{E}} - \sigma_{\mathbf{v}\uparrow\uparrow\mathbf{E}}}{\sigma_{\mathbf{v}\uparrow\downarrow\mathbf{E}} + \sigma_{\mathbf{v}\uparrow\uparrow\mathbf{E}}} \cong \frac{I^- - I^+}{I^- + I^+} \cong \frac{\sigma_{\mathrm{He}\to\mathrm{NO}} - \sigma_{\mathrm{He}\to\mathrm{ON}}}{\sigma_{\mathrm{He}\to\mathrm{NO}} + \sigma_{\mathrm{He}\to\mathrm{ON}}} \equiv S_{i\to f}. \quad (10)$$

The relationship of the experimental quantity SA with the molecular steric effect $S_{i\to f}$ requires knowledge of which end of the NO molecule is selected in the collision frame. This in turn enables comparison with the calculations of the steric effect, which should yield $S_{i\to f}$ directly. The identification in Eq. (10) uses the directly measured orientation of the applied static field and the sign of the dipole moment from *ab initio* calculations, $N^{\delta-}O^{\delta+}$,[42] and assumes no long-range collision-induced reorientation. As will be seen below, this assignment results in a disagreement of a factor of -1 between theory and experiment. The statistical spread in the individual measurements of the steric effect (i.e., the 12–15 cycles of the orientation of the applied field) is used to derive the experimental precision of the determination of SA.

The measurement of the zero-field signal, proportional to the scattering from the selected pure $\epsilon=-1$ state, can be combined with the orientation measurements to derive the relative state-to-state inelastic cross sections from individual Λ-doublet levels. The average of the signals at the two orientations is proportional to the average of the cross sections for scattering from the two initial Λ-doublet states:

$$I^- + I^+ \propto \alpha^2 \sigma_{\epsilon=-1\to|j'\Omega'\epsilon'\rangle} + \beta^2 \sigma_{\epsilon=1\to|j'\Omega'\epsilon'\rangle}. \quad (11)$$

Combining this with the measured zero-field signal, $I^0 \propto \sigma_{\epsilon=-1|\to|j'\Omega'\epsilon'\rangle}$, and assuming that the apparatus function does not change with applied dc field (i.e., the proportionality constants are equal), the ratio of cross sections from the different initial Λ-doublet states to the probed final state can be estimated as

$$\frac{I^- + I^+}{I^0} = \frac{\alpha^2 \sigma_{\epsilon=-1\to|j'\Omega'\epsilon'\rangle} + \beta^2 \sigma_{\epsilon=+1\to|j'\Omega'\epsilon'\rangle}}{\sigma_{\epsilon=-1\to|j'\Omega'\epsilon'\rangle}}, \quad (12)$$

$$L_{\epsilon'} \equiv \frac{\sigma_{\epsilon=+1\to|j'\Omega'\epsilon'\rangle}}{\sigma_{\epsilon=-1\to|j'\Omega'\epsilon'\rangle}} = \frac{\dfrac{I^- + I^+}{I^0} - \alpha^2}{\beta^2}. \quad (13)$$

The derived ratio of Λ-doublet cross sections, $L_{\epsilon'}$, is least reliable near $L_{\epsilon'}=0$. For values of $(I^- + I^+)/I^0$ close to α^2, $L_{\epsilon'}$ is very sensitive to inaccuracies in the computed mixing coefficients and to possible inhomogeneities in the orientation field. A 10% error in the square of the mixing coefficient would correspond to an uncertainty in the ratio of cross sections of ~ 0.4 near $L_{\epsilon'}=0$.

IV. RESULTS AND DISCUSSION

A. Calculated integral and differential cross sections

Predicted integral cross sections for $E_{tr}=508\,\mathrm{cm}^{-1}$ are presented in Fig. 3 together with the experimental data from Joswig *et al.*[10] The absolute value of the integral cross sections was estimated by Joswig *et al.*[10] from a comparison to the total attenuation of the primary beam. In Fig. 3, the experimental results are scaled to the total calculated cross section, i.e., the sum of the experimental cross sections matches the sum of the calculated cross sections on the RCCSD(T) surface. The agreement is quite satisfactory for both spin-orbit conserving and spin-orbit changing collisions. The RCCSD(T) and the CEPA surfaces give slightly different branching between the $F_1\to F_1$ and $F_1\to F_2$ scattering, with the RCCSD(T) results in closer agreement with the experiment; however, the shapes of the final j' distributions are very similar for the two surfaces. The differential cross sections (DCS) for the spin-orbit conserving transition from j

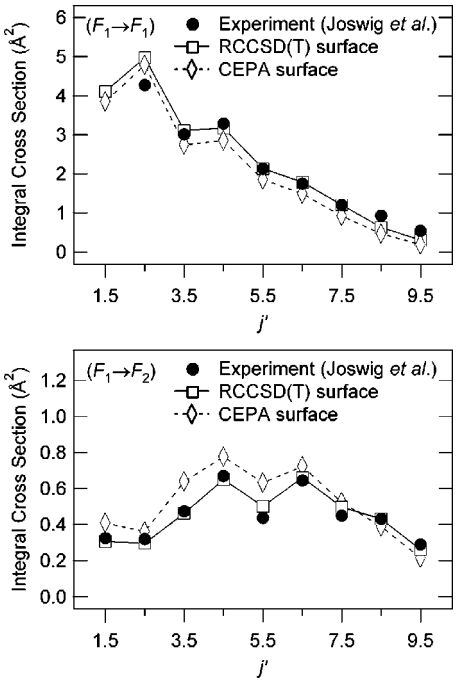

FIG. 3. Comparison of the calculated and experimental (Ref. 10) integral cross sections for scattering of NO $F_1(j=0.5)$ by He at $E_{tr}=508\,\mathrm{cm}^{-1}$ into final rotational states j' of the F_1 and F_2 manifolds. The experimental results are scaled so that the sum of the experimental cross sections matches the sum of the calculated cross sections on the RCCSD(T) (Ref. 35) surface.

$=0.5$ to final state $j'=3.5$ at $E_{tr}=491\,\mathrm{cm}^{-1}$, calculated using the RCCSD(T) (Ref. 35) and CEPA (Ref. 34) surfaces, are shown in Fig. 4. The results are compared to the experimental results of Westley *et al.*[28] The results on the RCCSD(T) surface show a maximum in the differential cross section closer to the experimental maximum than do the calculations on the CEPA PES. However, calculations on both surfaces predict the maximum at larger scattering angles. The experimental maximum of the DCS occurs at $\approx\vartheta=45°$, and the RCCSD(T) maximum is near 50°. The differential cross section on the CEPA surface has its maximum at 60°. Westley *et al.*[28] reported this same discrepancy between calculated scattering on the Yang and Alexander[34] CEPA potential and the experimental DCS. Based on a fit of their experimental rainbow maxima results to scattering from a hard ellipsoid model potential, they suggested that the repulsive core in the CEPA surface was insufficiently anisotropic. The anisotropy of the repulsive part of the RCCSD(T) sum potential is greater than that on the CEPA PES, and the maximum in the DCS for scattering on the RCCSD(T) surface is indeed closer to the experimental value.

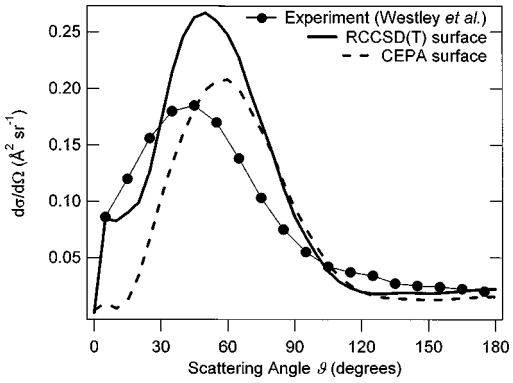

FIG. 4. Differential cross sections for scattering from the $F_1(j=0.5)$ state into the $F_1f(j'=3.5)$ state in collisions with He at $E_{tr}=491\,\mathrm{cm}^{-1}$, calculated on the RCCSD(T) (Ref. 35) (solid line) and CEPA (Ref. 34) (dashed line) surfaces, compared to the experimental measurements of Westley *et al.* (Ref. 28) (filled circles).

B. Steric effects and Λ-doublet propensities for $F_1 \rightarrow F_1$ transitions

The experimental and calculated steric asymmetries $(\mathrm{SA}, S_{i\rightarrow f})$ and Λ-doublet propensities $(L_{\epsilon'})$ for transitions to the F_1 state are given in Table I. The experimental uncertainties in Table I represent $\pm 1\sigma$ precision based on the statistical uncertainty in the steric effect determination, and do not include possible systematic errors, such as inhomogeneities in the orientation field or errors in the assumed mixing coefficients. Where several experiments have been performed for a final rotational state, the individual values and uncertainties are listed.

The highest final rotational state detected is $j'=12.5$, with a rotational energy of $E_{rot}=281\,\mathrm{cm}^{-1}$, well below the nominal translational energy of 514 cm^{-1}. By comparison, experiments in which NO$(j=0.5)$ scattered from Ar at similar collision energy detected rotational states up to 16.5.[6] This phenomenon was also noted in previous scattering experiments[8,26,28] and attributed to an angular momentum constraint on the rotational energy disposal.[8] This constraint may indicate that the anisotropy of the He-NO potential surfaces[34,35] is too weak to achieve a facile (classically allowed) conversion of all translational energy to rotational energy.[43]

The steric asymmetry for scattering into the *e* and *f* levels of the F_1 manifold is plotted in Fig. 5. As in the case of NO-Ar scattering, the steric asymmetry exhibits a striking oscillation with the change in rotational quantum number Δj. The "phase" of the oscillation is the same as in NO-Ar,[5] i.e., SA is negative for odd Δj and positive for even Δj. However, the amplitude of the oscillations is much larger for NO-He than for NO-Ar, which supports the suggestion of Alexander and Stolte[23] that the alternation in steric asymmetry originates from scattering off the repulsive shell. The interaction of NO with He is considerably less attractive $[D_e(\mathrm{NO\text{-}He})\sim 25\,\mathrm{cm}^{-1}]$ (Ref. 35) than NO with Ar $[D_e(\mathrm{NO\text{-}Ar})\sim 116\,\mathrm{cm}^{-1}]$.[18] Scattering into *f* states shows smaller absolute values of the steric asymmetry than scattering into *e* states for nearly all j'.

The calculated steric asymmetries for both the RCCSD(T) and CEPA surfaces are also shown in Fig. 5. The calculations agree well with the measurements, except for the absolute sign of the steric asymmetry. The comparison of the sign of the experimental steric effect with calculated steric effects remains somewhat open to question.[24] The sign of the experimental steric effect SA is fixed by directly measuring the applied voltages and spectroscopically establishing that the low-field seeking Λ-doublet state is preserved in the scattering center.[24] The sign of the steric asymmetry $S_{i\rightarrow f}$ in the calculations depends on the definition of the coordi-

TABLE I. Steric asymmetries and Λ-doublet propensities for $F_1 \rightarrow F_1$ scattering. Uncertainty estimates reflect the precision of the individual determinations and do not include possible systematic errors.

		Steric asymmetry			Λ-doublet propensity		
j'	ϵ'	Experiment SA ($\pm 1\sigma$)	RCCSD(T) $S_{i\rightarrow f}$	CEPA $S_{i\rightarrow f}$	Experiment $L_{\epsilon'}(\pm 1\sigma)$	RCCSD(T) $L_{\epsilon'}$	CEPA $L_{\epsilon'}$
1.5	1	−0.082±0.009	0.0604	0.0432	0.70±0.06	0.5506	0.4518
1.5	1	−0.060±0.009			0.65±0.06		
1.5	−1	0.03±0.01	0.1001	0.0861	1.9±0.2	1.9009	2.3387
2.5	1	0.166±0.007	−0.2075	−0.2219	3.23±0.09	3.9405	4.7811
2.5	1	0.20±0.01			3.2±0.2		
2.5	−1	0.092±0.005	−0.0755	−0.0715	0.52±0.05	0.2594	0.2131
3.5	1	−0.070±0.006	0.1274	0.121	0.77±0.04	0.7732	0.6835
3.5	−1	−0.097±0.008	0.1602	0.1687	1.7±0.1	1.3275	1.5118
4.5	1	0.400±0.007	−0.4163	−0.4548	2.38±0.08	2.1753	2.3983
4.5	1	0.398±0.005			2.3±0.1		
4.5	−1	0.280±0.008	−0.2328	−0.2384	⋯	0.4904	0.4522
5.5	1	−0.381±0.007	0.3800	0.4065	1.24±0.06	1.3015	1.1866
5.5	1	−0.323±0.007			1.01±0.08		
5.5	−1	−0.391±0.006	0.3167	0.3562	1.11±0.07	0.7484	0.8173
6.5	1	0.570±0.009	−0.4470	−0.4454	1.5±0.1	1.3664	1.6735
6.5	−1	0.43±0.04	−0.3368	−0.2824	0.38±0.15	0.7766	0.6553
6.5	−1	0.492±0.007			0.72±0.08		
6.5	−1	0.42±0.01			0.83±0.10		
7.5	1	−0.66±0.01	0.6334	0.6322	⋯	2.1606	1.9475
7.5	−1	−0.484±0.008	0.3713	0.4067	⋯	0.4799	0.5307
7.5	−1	−0.500±0.007			0.51±0.08		
7.5	−1	−0.48±0.01			0.70±0.09		
8.5	1	0.52±0.01	−0.4334	−0.3865	⋯	1.4756	2.4577
8.5	−1	0.30±0.01	−0.2318	−0.1241	0.69±0.07	0.6311	0.4443
8.5	−1	0.30±0.02			0.6±0.1		
9.5	1	−0.49±0.03	0.7334	0.6887	1.9±0.3	2.9224	2.2983
9.5	−1	−0.49±0.02	0.3940	0.4392	0.8±0.1	0.4613	0.6532
10.5	1	0.45±0.03	−0.5007	−0.0890	1.3±0.4	2.3874	4.6323
10.5	1	0.43±0.03			1.8±0.3		
10.5	−1	0.09±0.05	−0.0469	0.1148	0.3±0.3	0.2329	0.3224
11.5	1	−0.5±0.1	0.5274	0.0818	2.3±1.4	4.3352	0.7603
11.5	−1	−0.33±0.09	0.5073	0.3407	⋯		
12.5	1	−0.42±0.08			0.7±0.7	0.354	
12.5	1	0.2±0.1			1.7±1.2		

nates of the collision frame. The two quantities can be related by using the calculated direction of the NO dipole moment,[42] which causes the sign of the experimentally derived steric effect to oppose that of the calculations.[24] A resolution of the sign disagreement remains elusive; for the present comparisons, the calculated steric asymmetries are referenced to the right axis, which is simply the left axis multiplied by −1, to emphasize the agreement of the calculated magnitude with the experimental determination. The calculations on both surfaces reproduce the alternation in SA with even and odd Δj. The RCCSD(T) surface gives a larger magnitude of the steric asymmetry at high Δj than does the CEPA surface, in better agreement with experiment. This difference may be attributable to the greater anisotropy of the repulsive core in the RCCSD(T) potential.

The dependence of the ratio $L_{\epsilon'}$ for the spin-orbit manifold conserving collisions is displayed in Fig. 6 for outgoing *e* and *f* levels. The computed Λ-doublet propensities are in relatively good agreement with the experimental determinations. The calculations on the RCCSD(T) surface match the experimental values slightly more closely than those on the CEPA surface for high Δj. Because NO($^2\Pi_{1/2}$) is well described by Hund's case (a) for low *j*, the inelastic cross section should be unchanged upon reversing the parity index of both initial and final states.[44] This invariance in turn implies the following relationship:

$$L_{\epsilon'=1} = L_e = \frac{\sigma_{j,e\rightarrow j',e}}{\sigma_{j,f\rightarrow j',e}} = \frac{\sigma_{j,f\rightarrow j',f}}{\sigma_{j,e\rightarrow j',f}} = (L_{\epsilon'=-1})^{-1}. \quad (14)$$

That is, in the Hund's case (a) limit the values of $L_{\epsilon'}$ for outgoing *e* and *f* levels should be reciprocal. Both experimental and theoretical data obey Eq. (14) reasonably well for spin-orbit conserving transitions.

For $\Delta j \leqslant 6$ there appears to be a preference for overall parity $[p=\epsilon(-1)^{j-1/2}]$ conservation, i.e., $L_{\epsilon'}>1$ for odd Δj transitions to *f* levels and for even Δj transitions to *e* levels, $L_{\epsilon'}<1$ otherwise. Parity conservation has also been observed by Drabbels *et al.* in collisions of NO ($v=20$, $j=0.5$) with He.[33] The parity conserving transitions are facilitated by even *l* terms in the angular expansion of the potential energy surface [Eq. (4)],[45] and so are a manifestation of the "nearly homonuclear" character of NO. For $\Delta j>6$ the Λ-doublet quantum number is preferentially preserved, with

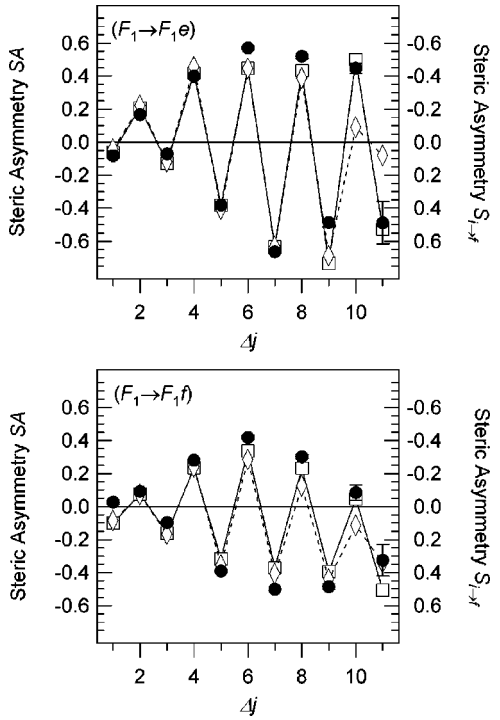

FIG. 5. Steric asymmetries for inelastic scattering from $F_1(j=0.5)$ into final rotational states $F_1(j',\epsilon')$. The present experimental values for SA (●) are referenced to the left axis, and calculations of $S_{i\rightarrow f}$ on the RCCSD(T) surface (Ref. 35) (□) and on the CEPA surface (Ref. 34) (◇) are referenced to the right axis.

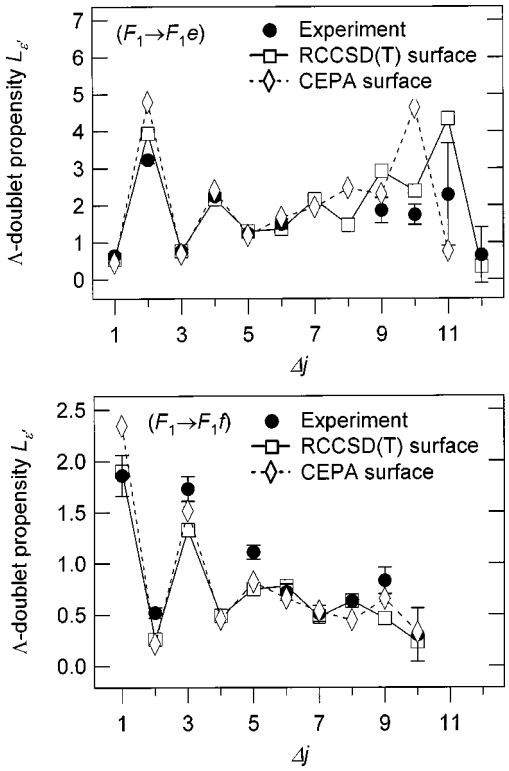

FIG. 6. Ratio of initial Λ-doublet cross sections for inelastic scattering from $F_1(j=0.5)$ into final rotational states $F_1(j',\epsilon')$: present experimental values (●), calculations on the RCCSD(T) surface (Ref. 35) (□), and calculations on the CEPA surface (Ref. 34) (◇).

$\sigma_{e\rightarrow\epsilon'=\epsilon} > \sigma_{e\rightarrow\epsilon'=-\epsilon}$, or $L_{\epsilon'}>1$ for $\epsilon'=1\,(e)$ states and $L_{\epsilon'}<1$ for $\epsilon'=-1\,(f)$ states. A propensity for overall parity conservation may also be manifested in the steric asymmetries. In the Hund's case (a) limit, suited to the $j=0.5$ initial state, the numerator in the expression for the steric asymmetry, $(\sigma_{\mathrm{He}\rightarrow\mathrm{NO}}-\sigma_{\mathrm{He}\rightarrow\mathrm{ON}})$, should not change with the outgoing Λ-doublet level,[23] and $(\sigma_{\mathrm{He}\rightarrow\mathrm{NO}}-\sigma_{\mathrm{He}\rightarrow\mathrm{ON}})$ will depend only on Δj, not on ϵ. Because the degree of mixing of the initial state in the electric orientation field is relatively low ($\beta^2=0.221$), Eq. (10) suggests that for pure case (a) molecules if $L_{\epsilon'}>1$, then $\mathrm{SA}_{\epsilon'}>\mathrm{SA}_{-\epsilon'}$ and if $L_{\epsilon'}<1$, then $\mathrm{SA}_{\epsilon'}<\mathrm{SA}_{-\epsilon'}$. A propensity for overall parity conservation further implies that the overall (orientation averaged) cross section for scattering out of the field-induced state, $(\sigma_{\mathrm{He}\rightarrow\mathrm{NO}}+\sigma_{\mathrm{He}\rightarrow\mathrm{ON}})/2$, will be larger for states with the same overall parity as the hexapole selected ($j=0.5$, $\epsilon=-1$) state. Thus, the magnitude of SA will be greater for final *e* states than for *f* states when Δj is even and |SA| will be greater for *f* states when Δj is odd, if parity conservation in the outgoing state prevails and the Hund's case (a) coupling is appropriate.

C. Steric effects and Λ-doublet propensities for $F_1 \rightarrow F_2$ transitions

The steric asymmetries and Λ-doublet propensities for spin-orbit manifold changing transitions ($F_1 \rightarrow F_2$) are given in Table II. The dependence of the steric asymmetry on the final rotational state is plotted in Fig. 7. Overall, N-end collisions are calculated to be more likely to produce a change in the spin-orbit level. The dependence of the steric asymmetry upon the Λ-doublet component in the outgoing state is smaller in ($F_1 \rightarrow F_2$) than in ($F_1 \rightarrow F_1$) scattering, suggesting a tendency for parity breaking transitions. Comparison of the upper and lower panels of Fig. 7 reveals that the overall preference for N-end collisions compared to O-end collisions is greater for $F_2 e$ than for $F_2 f$ outgoing states. As earlier calculated by Yang and Alexander[34] the $F_2 e$ states, which correlate with departure along the A'' PES, are favored in an $F_1 \rightarrow F_2$ transition, and $F_1 f$ is preferred over $F_1 e$ when the spin-orbit state is conserved.

The steric asymmetry exhibits an oscillatory behavior with the same phase as observed for the spin-orbit conserving NO-He collisions. For $4 \leqslant \Delta j \leqslant 10$ (except for scattering to the *f* level of $j'=10.5$) the sign of the steric effect appears to depend simply on whether Δj is odd or even. By comparison, the steric asymmetry for spin-orbit manifold changing NO-Ar collisions shows significantly attenuated alternations with Δj.[22,23,41,46] For NO-He the alternation is equally strong for ($F_1 \rightarrow F_2$) and ($F_1 \rightarrow F_1$) scattering, perhaps because of the dominance of repulsive interactions in the rotational energy transfer. The agreement between calculated and experimental steric asymmetries is slightly worse for the spin-orbit changing collisions than for the spin-orbit conserving collisions. Because the change in spin-orbit state is governed by the difference potential, the discrepancy in the steric asymmetry may arise from inaccuracies of the difference potential. For NO-Ar the difference potential has been thought to be less reliable than the sum potential.[16,17]

The dependence of the cross section on the incoming

TABLE II. Steric asymmetries and Λ-doublet propensities for $F_1 \rightarrow F_2$ scattering. Uncertainty estimates reflect the precision of the individual determinations and do not include possible systematic errors.

		Steric asymmetry			Λ-doublet propensity		
j'	ϵ'	Experiment SA ($\pm 1\sigma$)	RCCSD(T) $S_{i\rightarrow f}$	CEPA $S_{i\rightarrow f}$	Experiment $L_{\epsilon'}(\pm 1\sigma)$	RCCSD(T) $L_{\epsilon'}$	CEPA $L_{\epsilon'}$
1.5	1	−0.12±0.02	0.0628	0.0608	1.9±0.2	5.2371	0.0554
1.5	−1	⋯	0.3668	0.3542	⋯	13.8044	13.2418
2.5	1	−0.09±0.02	0.0661	0.0843	1.9±0.2	0.7528	0.9205
2.5	−1	−0.03±0.03	0.1985	0.1857	2.4±0.3	1.8771	1.4766
3.5	1	−0.17±0.02	0.1459	0.1158	−0.2±0.1	0.2556	0.0934
3.5	−1	−0.22±0.02	0.363	0.3384	1.7±0.1	4.5743	5.9394
4.5	1	0.13±0.01	−0.1081	−0.1538	0.43±0.06	0.4388	0.5471
4.5	−1	0.14±0.02	−0.1306	−0.2018	4.2±0.3	2.8428	2.1383
5.5	1	−0.41±0.02	0.4474	0.3979	0.8±0.2	1.1511	0.8953
5.5	1	−0.45±0.01			1.2±0.1		
5.5	−1	−0.46±0.02	0.3638	0.4097	2.5±0.2	0.9258	1.2156
6.5	1	0.17±0.01	−0.0790	−0.1308	−0.4±0.1	0.3118	0.4174
6.5	−1	0.13±0.01	−0.2252	−0.3051	10.6±0.6	4.1141	2.8998
7.5	1	−0.51±0.01	0.5751	0.5590	0.28±0.15	1.9187	1.5286
7.5	−1	−0.52±0.01	0.3036	0.3557	0.8±0.1	0.4678	0.6143
8.5	1	0.11±0.01	−0.0548	−0.0957	0.25±0.06	0.3811	0.5222
8.5	−1	0.14±0.03	−0.2349	−0.2683	5.7±0.6	3.5774	2.4648
8.5	−1	0.10±0.01			8.5±0.4		
9.5	1	−0.49±0.01	0.5202	0.5473	3.0±0.2	2.2981	1.9457
9.5	−1	−0.34±0.02	0.2318	0.2855	0.3±0.1	0.3682	0.4416
9.5	−1	−0.38±0.02			0.3±0.1		
10.5	1	0.10±0.02	−0.0673	−0.1058	0.5±0.1	0.5587	0.8585
10.5	−1	0.12±0.03	−0.2097	−0.2352	3.2±0.4	2.4998	1.6668
11.5	1	−0.25±0.04	0.4148	0.4943	2.5±0.5	2.7536	2.8755
11.5	−1	−0.23±0.03	0.1416	0.1947	0.5±0.2	0.3038	0.2721

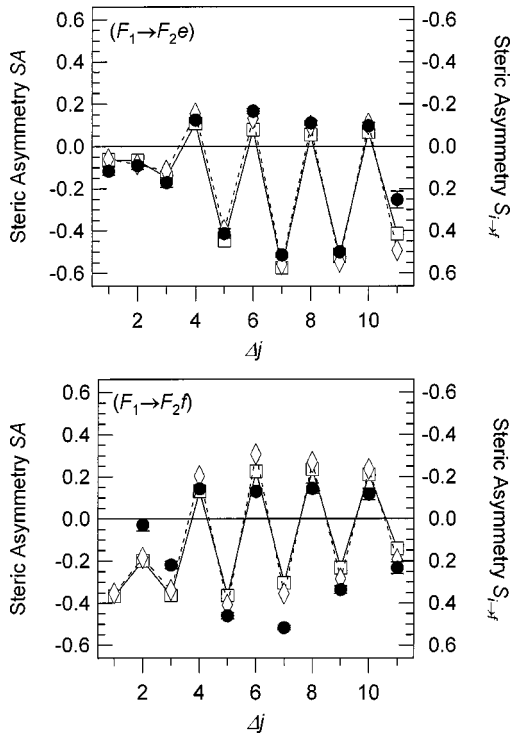

FIG. 7. Steric asymmetries for inelastic scattering from $F_1(j=0.5)$ into final rotational states $F_2(j',\epsilon')$. The present experimental values for SA (●) are referenced to the left axis, and calculations of $S_{i\rightarrow f}$ on the RCCSD(T) surface (Ref. 35) (□) and on the CEPA surface (Ref. 34) (◇) are referenced to the right axis.

Λ-doublet component, $L_{\epsilon'}$, is given in Table II and plotted against the final rotational state in Fig. 8. The apparent experimental ratios for scattering into the *e* states with $\Delta j=3$ and $\Delta j=6$ are negative, a nonphysical result for positive cross sections. As discussed above, for $(I^- + I^+)/I^0$ close to α^2, the effect of systematic uncertainty in the mixing parameters, which is not included in the stated precision, can be significant. These negative ratios are therefore best interpreted as $L_{\epsilon'} \ll 1$. Note the widely different values for $L_{\epsilon=1}(j'=1.5)$ predicted by calculations on the CEPA and RCCSD(T) surfaces. Comparison with experiment for this transition must also account for final-state mixing of the Λ-doublet levels by the orientation field. This effect, which is expected to be significant only for $F_2 j=1.5$, has not been included in the present analysis. In all other cases the results on the CEPA and RCCSD(T) surfaces agree rather well. For $\Delta j \leqslant 4$, parity conservation plays at most a minor role. For $\Delta j \geqslant 6$ the scattering exhibits a propensity for total parity changing collisions. For the highest final states, $\Delta j \geqslant 9$, the ratios $L_{\epsilon'}$ for outgoing *e* levels are nearly equal to the reciprocals of the ratios for outgoing *f* levels. The calculations are in qualitative agreement with the experimental determinations.

Transitions that preserve the overall parity are governed by terms of even angular symmetry in the potential energy surface.[45] A preference for parity changing in the spin-orbit changing collisions is directly explicable from inspection of the potentials in Fig. 1. Whereas $F_1 \rightarrow F_1$ scattering is gov-

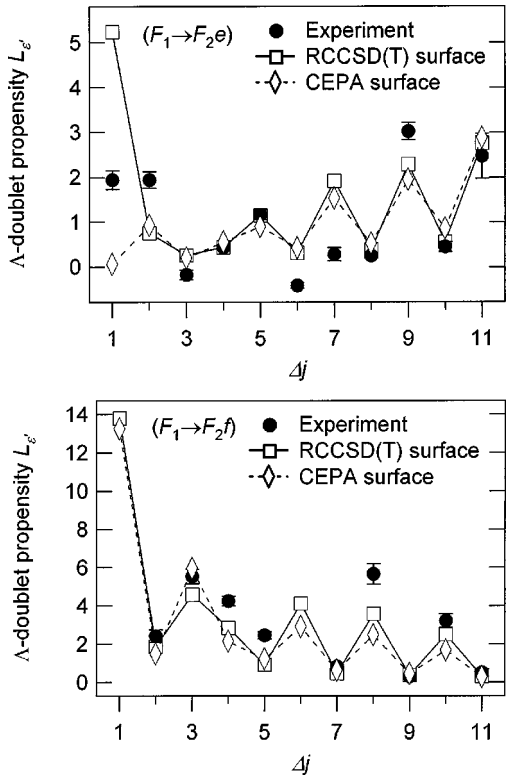

FIG. 8. Ratio of initial Λ-doublet cross sections for inelastic scattering from $F_1(j=0.5)$ into final rotational states $F_2(j',\epsilon')$: present experimental values (●), calculations on the RCCSD(T) surface (Ref. 35) (□), and calculations on the CEPA surface (Ref. 34) (◇).

erned by $V_{1,1}$, the $F_1 \rightarrow F_2$ transitions are induced by $V_{1,-1}$. The $V_{1,-1}$ surface displays a more heteronuclear angular dependence [i.e., more prominent odd-l terms in Eq. (4)] than does $V(1,1)$, which is more nearly homonuclear. The lack of parity conservation in the spin-orbit changing collisions for the NO-He system therefore suggests that these transitions are affected to a significant degree by odd-l terms in the difference potential.

V. CONCLUDING REMARKS

Steric asymmetries and Λ-doublet propensities have been measured for spin-orbit conserving and spin-orbit changing collisions of NO with He. The steric asymmetries for scattering into both spin-orbit states exhibit a prominent alternation in sign with Δj. This alternation is larger and more regular than that observed in previous studies of NO-Ar collisions, supporting earlier proposals[23] of a dominant role of scattering from the repulsive core in producing the alternation.

Comparison of scattering calculations with experiment shows that the RCCSD(T) potential energy surface of He-NO is reliable and is slightly better than the CEPA PES, but both surfaces give reasonable agreement with experiment. The agreement is slightly poorer for the spin-orbit changing collisions than for spin-orbit conserving collisions, which might suggest that the difference potential in both PESs is somewhat less accurate than the sum potential.

ACKNOWLEDGMENTS

The authors thank Professor Paul Houston (Cornell University) and Dr. David Chandler (Sandia National Laboratories) for raising our interest in open problems of the He-NO system. The Netherlands Organization for Scientific Research (NWO) is gratefully acknowledged for financial support through CW and FOM. C.A.T. is supported by the Division of Chemical Sciences, Geosciences, and Biosciences, the Office of Basic Energy Sciences, the U.S. Department of Energy, and his participation was partially facilitated by a NATO collaborative travel grant. Sandia is a multiprogram laboratory operated by Sandia Corporation, a Lockheed Martin Company, for the United States Department of Energy's National Nuclear Security Administration under Contract No. DE-AC04-94-AL85000. J.K. and A.A. acknowledge support from the European Research Training Network THEONET II.

[1] S. Stolte, J. Reuss, and H. L. Schwartz, Physica (Utrecht) **57**, 254 (1972).
[2] D. van den Ende and S. Stolte, Chem. Phys. Lett. **76**, 13 (1980).
[3] E. W. Kuipers, M. G. Tenner, A. W. Kleyn, and S. Stolte, Nature (London) **334**, 420 (1988).
[4] M. J. L. de Lange, J. J. van Leuken, M. M. J. E. Drabbels, J. Bulthuis, J. G. Snijders, and S. Stolte, Chem. Phys. Lett. **294**, 332 (1998).
[5] J. J. van Leuken, J. Bulthuis, S. Stolte, and J. G. Snijders, Chem. Phys. Lett. **260**, 595 (1996).
[6] M. J. L. de Lange, M. Drabbels, P. T. Griffiths, J. Bulthuis, S. Stolte, and J. G. Snijders, Chem. Phys. Lett. **313**, 491 (1999).
[7] J. J. van Leuken, F. H. W. van Amerom, J. Bulthuis, J. G. Snijders, and S. Stolte, J. Phys. Chem. **99**, 15573 (1995).
[8] P. A. Barrass, P. Sharkey, and I. W. M. Smith, Phys. Chem. Chem. Phys. **5**, 1400 (2003).
[9] P. Andresen, H. Joswig, H. Pauly, and R. Schinke, J. Chem. Phys. **77**, 2204 (1982).
[10] H. Joswig, P. Andresen, and R. Schinke, J. Chem. Phys. **85**, 1904 (1986).
[11] A. Lin, S. Antonova, A. P. Tsakotellis, and G. C. McBane, J. Phys. Chem. A **103**, 1198 (1999).
[12] C. R. Bieler, A. Sanov, and H. Reisler, Chem. Phys. Lett. **235**, 175 (1995).
[13] S. D. Jons, J. E. Shirley, M. T. Vonk, C. F. Giese, and W. R. Gentry, J. Chem. Phys. **105**, 5397 (1996).
[14] S. D. Jons, J. E. Shirley, M. T. Vonk, C. F. Giese, and W. R. Gentry, J. Chem. Phys. **97**, 7831 (1992).
[15] A. G. Suits, L. S. Bontuyan, P. L. Houston, and B. J. Whitaker, J. Chem. Phys. **96**, 8618 (1992).
[16] M. S. Elioff and D. W. Chandler, J. Chem. Phys. **117**, 6455 (2002).
[17] H. Kohguchi, T. Suzuki, and M. H. Alexander, Science **294**, 832 (2001).
[18] M. H. Alexander, J. Chem. Phys. **111**, 7426 (1999).
[19] E. A. Wade, K. T. Lorenz, D. W. Chandler, J. W. Barr, G. L. Barnes, and J. I. Cline, Chem. Phys. **301**, 261 (2004).
[20] K. T. Lorenz, D. W. Chandler, J. W. Barr, W. W. Chen, G. L. Barnes, and J. I. Cline, Science **293**, 2063 (2001).
[21] J. I. Cline, K. T. Lorenz, E. A. Wade, J. W. Barr, and D. W. Chandler, J. Chem. Phys. **115**, 6277 (2001).
[22] M. H. Alexander, Faraday Discuss. **113**, 437 (1999).
[23] M. H. Alexander and S. Stolte, J. Chem. Phys. **112**, 8017 (2000).
[24] A. Gijsbertsen, M. J. L. de Lange, A. E. Wiskerke, H. Linnartz, M. Drabbels, J. Klos, and S. Stolte, Chem. Phys. **301**, 293 (2004).
[25] C. W. McCurdy and W. H. Miller, J. Chem. Phys. **67**, 463 (1977).
[26] H. Meyer, J. Chem. Phys. **102**, 3151 (1995).
[27] H. Kim and H. Meyer, Chem. Phys. **301**, 273 (2004).
[28] M. S. Westley, K. T. Lorenz, D. W. Chandler, and P. L. Houston, J. Chem. Phys. **114**, 2669 (2001).
[29] M. Islam, I. W. M. Smith, and M. H. Alexander, Phys. Chem. Chem. Phys. **2**, 473 (2000).
[30] P. L. James, I. R. Sims, and I. W. M. Smith, Chem. Phys. Lett. **272**, 412 (1997).
[31] P. L. James, I. R. Sims, I. W. M. Smith, M. H. Alexander, and M. B. Yang, J. Chem. Phys. **109**, 3882 (1998).
[32] C. D. Ball and F. C. De Lucia, Chem. Phys. Lett. **300**, 227 (1999).

[33] M. Drabbels, A. M. Wodtke, M. Yang, and M. H. Alexander, J. Phys. Chem. A **101**, 6463 (1997).
[34] M. Yang and M. H. Alexander, J. Chem. Phys. **103**, 6973 (1995).
[35] J. Klos, G. Chalasinski, M. T. Berry, R. Bukowski, and S. M. Cybulski, J. Chem. Phys. **112**, 2195 (2000).
[36] W. B. Zeimen, G. C. Groenenboom, and A. van der Avoird, J. Chem. Phys. **119**, 131 (2003).
[37] W. B. Zeimen, G. C. Groenenboom, and A. van der Avoird, J. Chem. Phys. **119**, 141 (2003).
[38] J. W. C. Johns, J. Reid, and D. W. Lepard, J. Mol. Spectrosc. **65**, 155 (1977).
[39] M. G. Tenner, E. W. Kuipers, W. Y. Langhout, A. W. Kleyn, G. Nicolasen, and S. Stolte, Surf. Sci. **236**, 151 (1990).
[40] HIBRIDON is a package of programs for the time-independent quantum treatment of inelastic collisions and photodissociation written by M. H. Alexander, D. Manolopoulos, H.-J. Werner, and B. Follmeg, with contributions by P. Vohralik, G. Corey, B. Johnson, T. Orlikowski, and P. Valiron.
[41] M. J. L. de Lange, Ph.D. thesis, Vrije Universiteit, 2003.
[42] S. R. Langhoff, C. W. Bauschlicher, and H. Partridge, Chem. Phys. Lett. **223**, 416 (1994).
[43] D. Beck, U. Ross, and W. Schepper, Z. Phys. A **293**, 107 (1979).
[44] M. H. Alexander, J. Chem. Phys. **76**, 5974 (1982).
[45] A. Degli-Esposti, A. Berning, and H.-J. Werner, J. Chem. Phys. **103**, 2067 (1995).
[46] M. J. L. de Lange *et al.* (unpublished).